Indian Journal of Radio & Space Physics
Vol. 35, October 2006, pp. 327-334

Latitudinal and diurnal variations of some important atomic oxygen dayglow emissions

Arun Kr Upadhayaya[1], Vir Singh[2] & Satish Tyagi[3]

[1]Amity School of Engineering & Technology, Bijwasan , New Delhi 110 061, India

[2]Department of Physics, Indian Institute of Technology Roorkee, Roorkee 247 667, India

[3]BSNL Saharanpur, Uttar Pradesh

Email: akuphdph@iitr.ernet.in, virphfph@iitr.ernet.in

Received 23 June 2005; revised 13 January 2006; accepted 6 March 2006

In the present paper the latitudinal and diurnal variations of 5577 Å, 6300 Å, 7320 Å and 8446 Å dayglow emissions are presented. The volume emission rate profiles for these emissions are calculated using updated Glow model. To test the model, the calculated emission rate profiles for 5577 Å and 6300 Å are compared with the measurements of Wind Imaging Interferometer (WINDII) for which data are available. The emission intensities have been studied on 15 Jan. 1995 and 15 June 1995 using Tobiska solar EUV flux model. These calculations show that the intensity is maximum at 1200 hrs LT for both the dates at all latitudes for 5577 Å and 8446 Å emissions. The position of maximum intensity is found to be variable for 6300 Å emission on 15 January. At 30ºN latitude, the peak is found at 1000 hrs LT, while at 5ºN and 45ºN the maximum intensity is found to occur at nearly 1200 hrs LT. On 15 June, the intensity of 6300 Å emission does not show any pronounced peak and emission is found to vary within 15% between 0800 and 1400 hrs LT. On 15 January, the 7320Å emission shows that the peak of maximum intensity occurs at nearly 1200 hrs LT at 5ºN, which moves quite close to 1000 hrs LT at 30ºN and 45ºN latitudes. On the other hand, the peak of maximum intensity for 7320 Å emission is found between 1200 hrs and 1400 hrs LT at all latitudes on 15 June. The smooth variation in 8446 Å intensity may be attributed due to steadiness of photoelectron fluxes at higher energies.

Keywords: Dayglow emission, Atomic oxygen, Glow model, Solar EUV flux, Wind imaging interferometer
PACS No.: 94.10.Fa; 94.10.Rk; 94.10.Gb; 96.60 Rd
IPC Code: G01T1/11; G01M11/00

1 Introduction

Modelling of dayglow emissions has been carried out by several researchers[1-9] to understand the Middle Lower Thermosphere (MLT) dynamics. These studies have been carried out by studying various atomic oxygen emissions such as 5577 Å, 6300 Å, 7320 Å and 8446 Å either by means of observations or by modelling. The solar EUV flux plays a vital role in production of these emissions in dayglow. The production rates of these emissions are, hence, quite sensitive to the values of solar irradiance. Hinteregger *et al.*[10] and Tobiska[11] are, respectively, two referenced models that provide solar fluxes under different solar activity conditions. These solar flux models are based on the SC#21 REF solar minimum reference spectrum and flux variation measured by AE-E satellite. Inspite of the solar activity consideration these models have different scaling techniques and, therefore, give quite different solar EUV flux. The 5577 Å and 6300 Å dayglow emissions have been modelled by several researchers[1-6] using Hinteregger *et al.*[10] solar flux model. However, Hinteregger *et al.*'s[10] values are 24 years old. Many studies have pointed out that their values are about a factor of 1.5-2 lower than needed. This fact has also been confirmed by the SNOE satellite measurements[12] and TIMES satellite data will further confirm this fact. Tobiska's values are an extension and revision of Hinteregger *et al.*'s values based on the same Hinteregger *et al.*'s concept and the AE-data set. It may be noted that Tobiska's values are also about 1.5-2 higher than the Hinteregger *et al.*'s values. In view of these Tobiska[11] solar EUV flux model has been used in the present study.

The variations in atomic oxygen densities in E- and F-regions with the measurements are still a matter of concern to the modelers. The atomic oxygen plays a very important role in the study of atomic oxygen dayglow emissions. As such 5577 Å and 6300 Å emissions are widely studied. However, a very few studies have been reported for 7320 Å and 8446 Å emissions in dayglow[13-16]. The 7320 Å and the 8446 Å emissions are generated at higher altitudes (above

160 km), where atomic oxygen is major species. Hence, the study of these emissions can be used to infer information about the atomic oxygen densities in F- region. In this paper, the latitudinal and diurnal variations of 5577 Å, 6300 Å, 7320 Å and 8446 Å dayglow emissions in the northern hemisphere are presented. The analysis of these emissions is carried out using Glow model[17] by incorporating Tobiska[11] solar EUV flux model. The emission profiles so obtained using Tobiska[11] solar EUV flux model are then compared with the emission profiles measured[18] by Wind Imaging Interferometer (WINDII) on board Upper Atmosphere Research Satellite for 5577 Å and 6300Å emission to test the validity of the model. Unfortunately, no measurements are available for 7320 Å and 8446 Å dayglow emissions. The diurnal and latitudinal variations in emission intensities for 5577 Å, 6300Å, 7320 Å and 8446 Å are presented for two specific dates, i.e. on 15 Jan. 1995 and 15 June 1995 at a fixed longitude.

2 Model

In the Tobiska[11] model the solar EUV flux is scaled using parametrization method based on the Lyman-α slope for chromospheric fluxes and He-I 10830 Å equivalent width. This model also takes into account the daily 10.7 cm solar radio flux and its 81-day average flux. Tobiska[11] has used the following equations for scaling the solar flux.

$$\begin{aligned}SFLUX = {} & TCHRO + TCHR1\times HLYMOD \\ & + TCHR2\times HEIMOD + TCORO \\ & + TCOR1\times F107 + TCOR2\times F107A\end{aligned}$$

where,

TCHRO = Intercept of chromospheric fluxes, EUV 91 model
TCHR1 = H Lyman-α slope for chromospheric fluxes
TCHR2 = He fluxes 10830 Å equivalent width slope for chromospheric fluxes
TCOR0 = Intercept for coronal fluxes
TCOR1 = F10.7 slope for coronal fluxes
TCOR2 = F10.7A slope for coronal fluxes

$HLYMOD = HEIEW\times 3.77847\times 10^{9} + 8.40317\times 10^{10}$ (for HEIEW > 0.001)

$HLYMOD = 8.70E8\times F107 + 1.90\times 10^{11}$ (for HEIEW ≤ 0.001)

HLYMOD = HLYA (for HLYA > 0.001)

$HEIMOD = HEIEW\times 3.77847\times 10^{9} + 8.40317\times 10^{10}$ (for HEIEW > 0.001)

HEIMOD = HLYMOD (For HEIW≤ 0.001)

where,

HEIEW = He-I 10830 Å equivalent width
HLYA = H Lyman-α flux.

The values of the above parameters are listed in subroutine SSFLUX of Glow model.

Mechanisms of production of 5577 Å and 6300 Å have been discussed by several authors in detail[1,3,20]. Earlier studies[2,4,20] have shown that the photoelectron impact excitation and dissociative recombination processes mainly contribute towards the production of $O(^1S)$ and $O(^1D)$ in thermospheric region (160-220 km). However, the energy transfer by $N_2(A^3\sum_u^+)$ to atomic oxygen is important contributor to $O(^1S)$ production in the altitude region of 130-170 km, which is not found effective in $O(^1D)$ production. Photodissociation of molecular oxygen contributes effectively in the mesospheric altitude (100-120 km) in the daytime. The 8446 Å emission O(3*p*-3*s*) is mainly produced above 150 km in the sunlit atmosphere. The 8446 Å emission is produced by direct photoelectron impact on atomic and molecular oxygen. The minimum energy of a photon required to get $O^*(3p)$ from the photodissociation of O_2 will be the sum of dissociation energy of O_2 and excitation energy of atomic oxygen 3*p* state. This energy is higher than the ionization energy of O_2. Since this is the photon interaction process, the probability of O_2 ionization is much higher than the dissociative excitation of O_2 to the level of $O^*(3p)$. Link[21] has also discussed the production processes of $O^*(3p)$ state. The following photoelectron impact processes would produce the $O^*(3p)$ state.

$$O + e_{ph} \rightarrow O^*(3p) + e_{ph} \quad \ldots (1)$$

$$O_2 + e_{ph} \rightarrow O^*(3p) + O + e_{ph} \quad \ldots (2)$$

$$O^*(3p) \rightarrow O(3s) + h\nu\ (8446\ Å) \quad \ldots (3)$$

where, e_{ph} is the photoelectron and O(3*p*) is the excited atom of oxygen. Photoelectrons are produced by the interaction of solar ultraviolet radiation with the atmospheric neutral species (N_2, O_2, O).The production rates of 8446 Å emission due to processes (1) and (2) are calculated by using the same parameters as have been used by Singh[14]. The volume emission rates $V_1(z,\alpha)$ and $V_2(z,\alpha)$ at altitude *z* due to processes (1) and (2) are calculated by using the following expression, respectively

$$V_1(z,\alpha)= [O] \int_{E_{th}}^{\infty} \sigma_1(E)\phi(E,z,\alpha)\, dE \quad \ldots (4)$$

$$V_2(z,\alpha)= [O_2] \int_{E_{th}}^{\infty} \sigma_2(E)\phi(E,z,\alpha)\, dE \quad \ldots (5)$$

where, [O] and [O_2] are the densities of atomic and molecular oxygen, respectively, at altitude *z*, E_{th} the excitation threshold energy of O(3*p*) state, $\Phi(E,z,\alpha)$ the photoelectron flux which is a function of photoelectron energy *E*, altitude *z* and solar zenith angle α, and $\sigma_1(E)$ and $\sigma_2(E)$ are the emission cross-sections of 8446 Å due to processes (1) and (2), respectively. These cross-sections are taken from the work of Julienne and Daivs[22]. The MSIS-90 neutral model[22] atmosphere is used for the neutral densities. It would be important to mention here that this emission is an allowed transition and, therefore, the emission rate would be essentially the same as that of production rate. No collisional quenching will take place. The total volume emission rate at altitude *z* is the sum of $V_1(z,\alpha)$ and $V_2(z,\alpha)$

$$V(z,\alpha) = V_1(z,\alpha) + V_2(z,\alpha) \quad \ldots (6)$$

There are four emission lines (two pairs of doublets) associated with the 7320 Å emission $O^+(^2P$-$^2D)$. In the thermosphere, the major source of the $O^+(^2P)$ ion is the direct photoionization excitation of atomic oxygen caused by absorption of solar extreme ultraviolet photons with wavelengths less than 666 Å.

$$O + h\nu\ (\lambda < 666\ \text{Å}) \rightarrow O^+(^2P) + e \quad \ldots (7)$$

A secondary source is photoelectron impact ionization excitation of ground state oxygen atoms,

$$O + e_{ph} \rightarrow O^+(^2P) + 2e \quad \ldots (8)$$

where, e_{ph} is a photoelectron. The production rates due to processes (1) and (2) are obtained using the following expressions.

$$R_1(z, \alpha) = [O]\Sigma_\lambda\, I_z(\lambda, \alpha)\, \sigma_{O^+(^2P)}(\lambda) \quad \ldots (9)$$

$\lambda < 666$ Å

$$R_2(z, \alpha) = [O] \int_{E_{th}}^{\infty} \sigma_e(E)\, \phi(E, z, \alpha)\, dE \quad \ldots (10)$$

where $I_z(\lambda,\alpha)$ is the solar flux at wavelength λ and solar zenith angle α, [O] the atomic oxygen density, $\sigma_{O^+(^2P)}(\lambda)$ is the photoionization cross-section of $O^+(^2P)$ state, $\sigma_e(E)$ is the total excitation cross-section of $O^+(^2P)$ due to photoelectron of energy *E*. The total production rate of $O^+(^2P)$ is, therefore,

$$R(z, \alpha) = R_1(z, \alpha) + R_2(z, \alpha) \quad \ldots (11)$$

The $O^+(^2P)$ ions produced by photoionization and photoelectron ionization are lost through the following processes.

Radiative decay:

$$O^+(^2P) \xrightarrow{A_{12}} O^+(^2D, {}^4S) + h\nu\ (7320\ \text{Å}, 7330\ \text{Å}, 2470\ \text{Å}) \quad \ldots (12)$$

Quenching processes:

$$O^+(^2P) + e_{th} \xrightarrow{K_{13}} O^+(^4S) + e \quad \ldots (13)$$

$$O^+(^2P) + O \xrightarrow{K_{14}} O^+(^4S) + O \quad \ldots (14)$$

$$O^+(^2P) + N_2 \xrightarrow{K_{15}} O^+(^4S) + N_2 \quad \ldots (15)$$

The quenching factor is given by

$$Q_{O^+(^2P)} = \frac{A_{12}}{A_{12} + K_{13}[e] + K_{14}[O] + K_{15}[N_2]} \quad \ldots (16)$$

where, [e], [O] and [N_2] are the densities of thermal electrons, atomic oxygen and molecular nitrogen, respectively. The reactions and the rate coefficients are given in Table 1. The volume emission rate is, therefore, given by,

$$V(O^+(^2P)) = Q_{O^+(^2P)} * R(z, \alpha) \quad \ldots (17)$$

3 Results and discussion

The emission profiles for 5577 Å, 6300 Å, 7320 Å and 8446 Å dayglow emissions are obtained using Tobiska[11] solar EUV flux model. For the comparison purpose the volume emission rates (VER) of 5577 Å and 6300 Å are calculated for some specific cases for which WINDII data are available. In Fig. 1[(a) and (b)] volume emission rate profiles of 5577 Å have been shown for 13 Mar. 1994 at (26°S, 288°E) at

Table 1 — Reactions and rate coefficients

Reaction	Rate coefficients (cm^3s^{-1})	Reference No.
$O^+(^2P) + e_{th} \rightarrow O^+(^4S) + e_{th}$	$K_{13} = 1.89 \times 10^{-7}(300/T_e)^{0.5}$	15
$O^+(^2P) + O \rightarrow O^+(^4S) + O$	$K_{14} = 4.0 \times 10^{-10}$	15,24
$O^+(^2P) + N_2 \rightarrow O^+(^4S) + N_2$	$K_{15} = 3.4 \times 10^{-10}$	15,24
$O^+(^2P) \rightarrow O^+(^2D, ^4S) + h\nu(7320\ Å)$	$A_{12} = 0.17120$	21

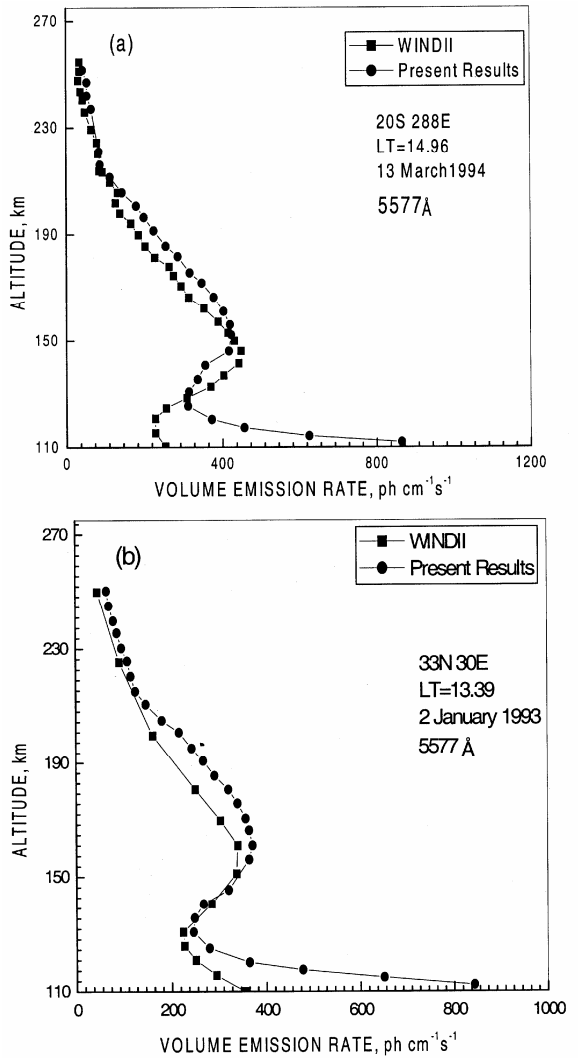

Fig. 1 — Comparison between volume emission rate profiles of 5577 Å emission obtained using present model and WINDII measurements for (a) 13 Mar. 1994 and (b) 2 Jan. 1993

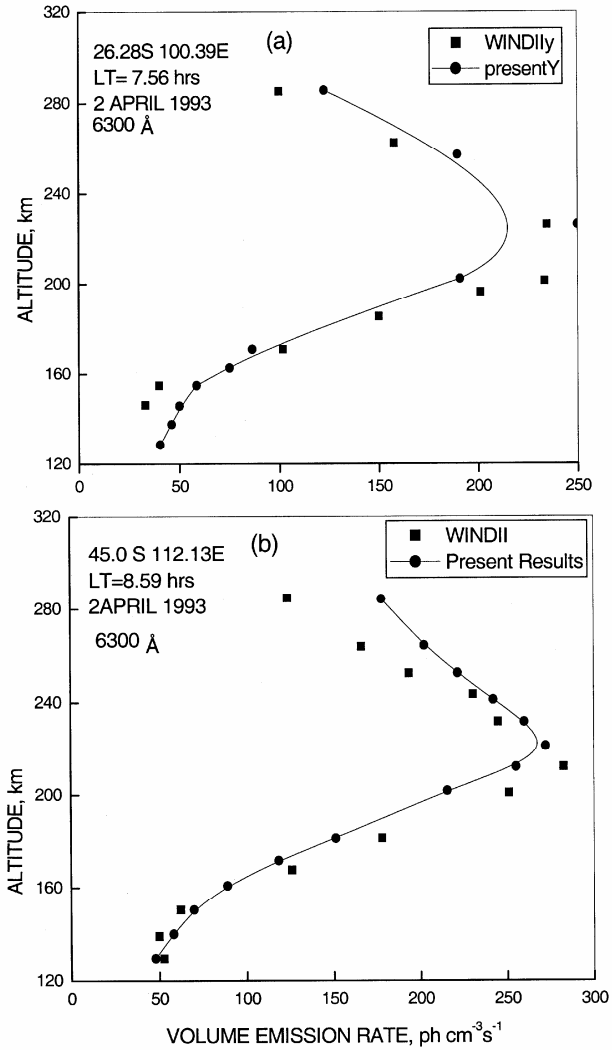

Fig. 2 — Comparison between volume emission rate profiles of 6300 Å emission obtained using present model and WINDII measurements at (a) 26.28°S, 100.39°E and (b) 45°S, 112.13°E

1496 hrs LT and on 2 Jan. 1993 at (30°N, 30°E) at 1339 hrs LT, respectively. The VERs are calculated using the updated temperature dependence rate coefficient for the reaction N_2 ($A^3\Sigma_u^+$) with atomic oxygen proposed by Hill *et al*.[25] with a quantum yield of 0.36 for this reaction, as incorporation of this value gives a better agreement[4] with the observations. It is noticeable from Fig. 1 that the profiles are in good agreement with WINDII observations above 130 km. Below this altitude the model underestimates the WINDII observations.

Figure 2[(a) and (b)] shows the calculated volume emission rate profiles of 6300 Å for 2 Apr. 1993 at (26.28°S, 100.39°E) at 0756 hrs LT and at (45°S,

112.13°E) at 0859 hrs LT along with WINDII measurements. It is noticed from Fig. 2[(a) and (b)] that between 160 and 220 km, the model results are in good agreement with the WINDII observations. The discrepancy between the present results and the measurements above 160 km for 5577 Å and above 220 km for 6300 Å emissions are possibly due to the fact that the Glow model does not take into account the transport of photoelectrons and atomic oxygen above 200 km. The inclusion of transport effect in the present model is a very difficult task and will be considered in future study. The above results show that the model values are in fairly good agreement with the observations. Thus, the Glow model can be used to study the 7320 Å and 8446 Å emissions. As such no measured emission rate profiles are available for 7320 Å and 8446 Å emissions from WINDII. Figure 3(a) shows the VER profile for 7320 Å on 1 Apr. 1994 at (26.28°S, 100.39°E) at 0756 hrs LT and Fig. 3(b) shows the VER profile for 8446 Å emission on 2 Apr.1993 at (45°S, 112.13°E) at 0859 hrs LT. The results are expected on the same line as obtained for 5577 Å and 6300 Å emissions.

To understand the diurnal and latitudinal variations of emission intensities, the calculations are made at various latitudes and local times in the northern hemisphere. The dates of 15 Jan. 1995 and 15 June 1995 have been chosen in the calculations, because these dates fully lie in winter and summer seasons, respectively. In Fig. 4[(a) and (b)] the variation of 5577 Å intensity as a function of local time is shown at (5ºN, 70ºE), (30ºN, 70ºE) and (45ºN, 70ºE) for 15 Jan. 1995 and 15 June 1995, respectively. It is noted from Fig. 4 that the maximum intensity is at local noontime (1200 hrs LT) at all latitudes for both the dates. However, 5577 Å intensity are significantly lower in the month of January at higher latitudes

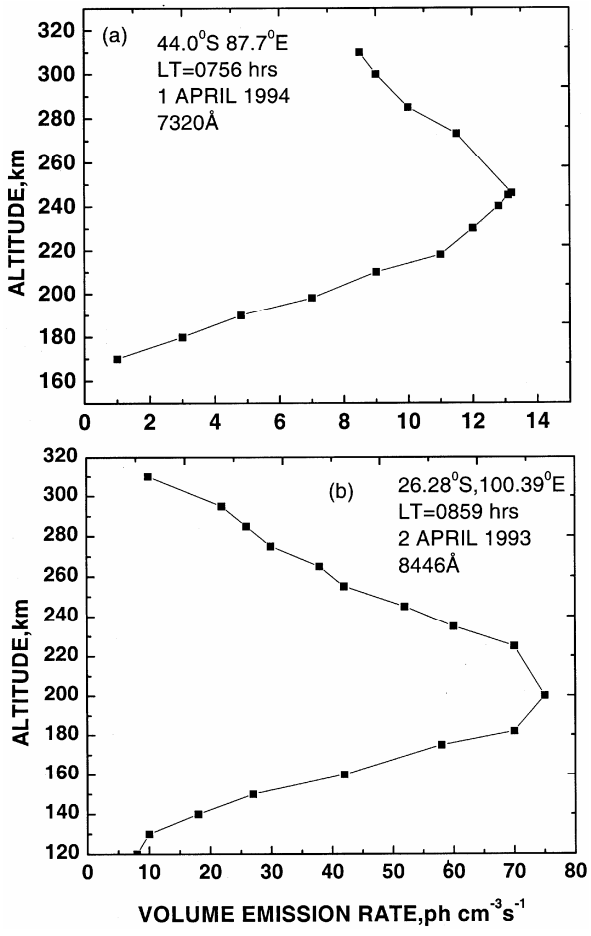

Fig. 3 — (a) Volume emission rate profile of 7320 Å emission obtained from the present model for 1 Apr. 1994 and (b) Volume emission rate profile of 8446 Å emission obtained from the present model for 2 Apr. 1993

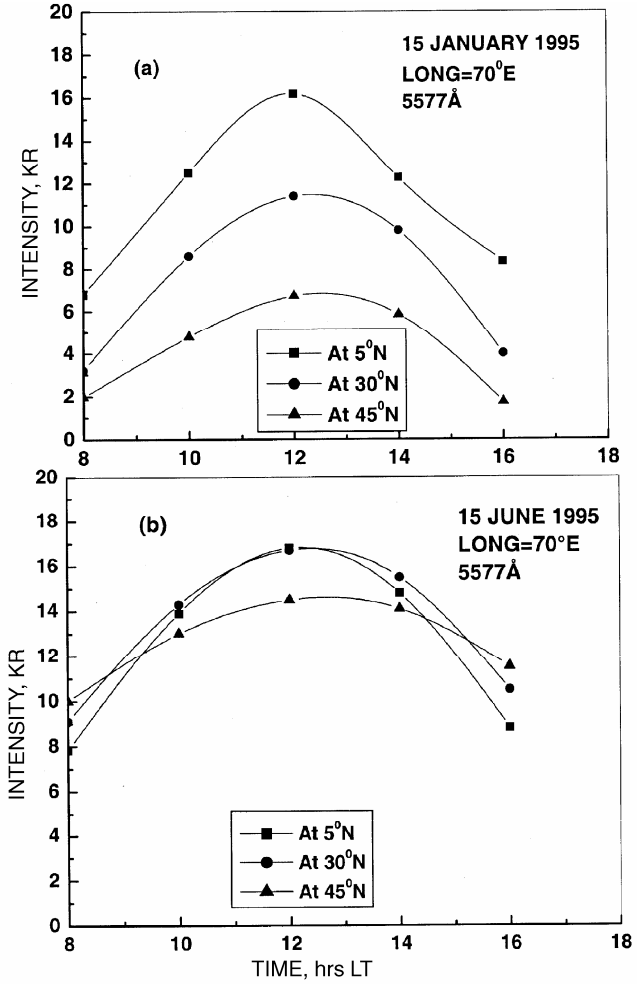

Fig. 4 — Variation of 5577 Å emission intensity as a function of local time at various latitudes for (a) 15 Jan. 1995 and (b) 15 June 1995

(30ºN, 45ºN) than the corresponding values in the month of June. This difference is mainly due to the solar zenith angle (SZA). In the month of January, at higher latitudes in the northern hemisphere solar zenith angle is much higher than the corresponding latitudes in the month of June. Higher solar zenith angle means more attenuation of solar radiation and less production of emission.

The variation of 6300 Å intensity as a function of local time is shown in Fig. 5[(a) and (b)] at (5°N, 70°E), (30ºN, 70ºE) and (45°N, 70°E) for 15 Jan. 1995 and 15 June 1995, respectively. It can be seen from Fig. 5[(a) and (b)] that the redline intensity shows large variations in the month of January, whereas for the month of June the intensity shows a very little variation with local time. In the month of June the intensity of 6300 Å shows only 15% variation between 0800 hrs and 1600 hrs LT and its value is found between 1.5 and 1.9 kR. In the month

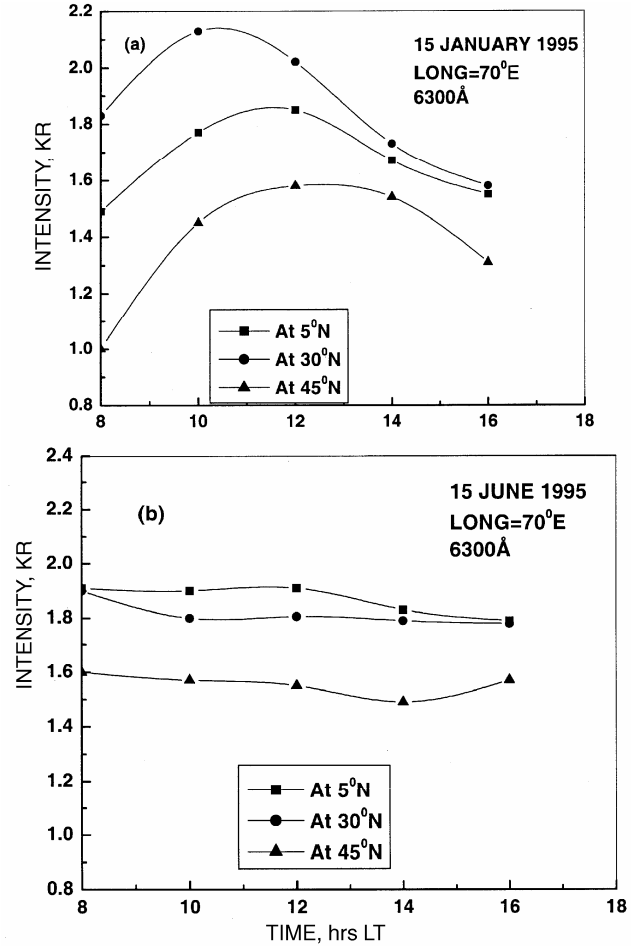

Fig. 5 — Variation of 6300 Å emission intensity as a function of local time at various latitudes for (a) 15 Jan. 1995 and (b) 15 June 1995

of January the 6300 Å intensity is found to be maximum at 30ºN latitude and peak is found at 1000 hrs LT. Sridharan *et al.*[26] have reported the measurements of intensity of 6300 Å dayglow emission at Waltair (17.7°N, 83.3°E) on 29 Jan.1993. The diurnal variation in intensity as reported by Sridharan *et al.*[26] is qualitatively similar to the present results. However, the absolute value of maximum intensity as reported by Sridharan *et al.*[26] is about 0.4 kR which is about four times smaller than the present values. It would be worthwhile to mention here that the present intensity results of 6300 Å dayglow emission are within 30% of agreement with the WINDII measurements. The WINDII measurements have been considered more reliable because these are based on better instrumentation and have been taken onboard Upper Atmosphere Research Satellite (UARS). At 5°N and 45°N, the maximum intensity is found to occur at nearly 1200 hrs LT. The variation in intensity is found about 70% between 0800 hrs and 1600 hrs LT. The reason to get more or less constant intensity in the month of June is that the SZA is smaller at all local times than in the month of January. Hence, the radiation penetrates deep into the atmosphere and O(^1D) is produced at lower altitudes. However, at lower altitudes the quenching of O(^1D) is very large and very little emission is produced at these altitudes. The main contributions to intensity come from higher altitudes and the integrated intensity is found to be more or less constant between 0800 and 1600 hrs LT in the month of June.

Figure 6[(a) and (b)] shows the variation of 7320 Å intensity as a function of local time at (5ºN, 70ºE), (30ºN, 70ºE) and (45ºN, 70ºE) for 15 Jan. 1995 and 15 June 1995, respectively. It is noted from Fig. 6(b) that the emission intensity shows flat peak between 1200 hrs and 1400 hrs LT for the month of June for 30ºN latitude. The variation in the intensity is found about 30% for the month of June. In January, 7320 Å emission shows large variation in the intensity, i.e. about 50%. It is clear from Fig. 6(a) that the peak of intensity at 5ºN latitude is at local noontime (1200 hrs) LT. However, at higher latitudes (30° and 45°N), the peak of intensity is found near 1000 hrs LT.

In Fig. 7[(a) and (b)] the variation of 8446 Å intensity as a function of local time is shown at (5ºN, 70ºE), (30ºN, 70ºE), and (45ºN, 70ºE) for 15 Jan. 1995 and 15 June 1995, respectively. It is noted from Fig. 7 that the variation of intensity is more or less qualitatively similar on both the dates. However, in the morning hours the intensity of 8446 Å emission is

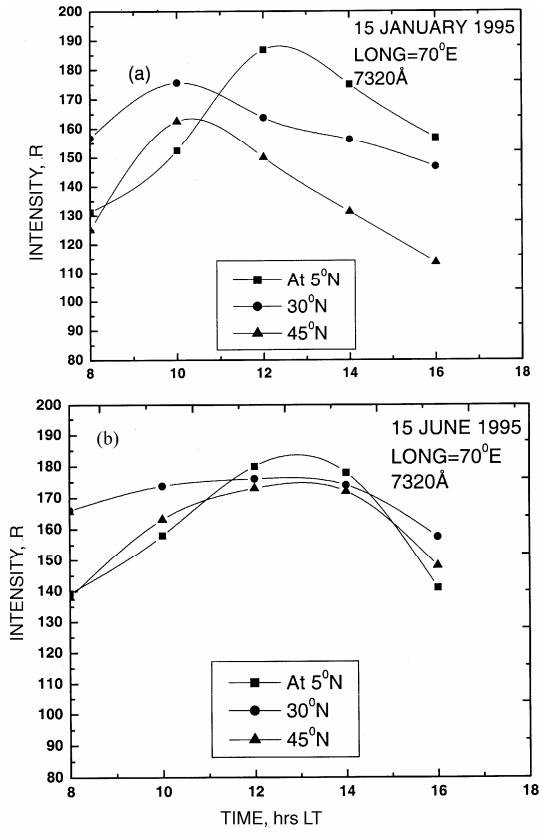

Fig. 6 — Variation of 7320 Å emission intensity as a function of local time at various latitudes for (a) 15 Jan. 1995 and (b) 15 June 1995

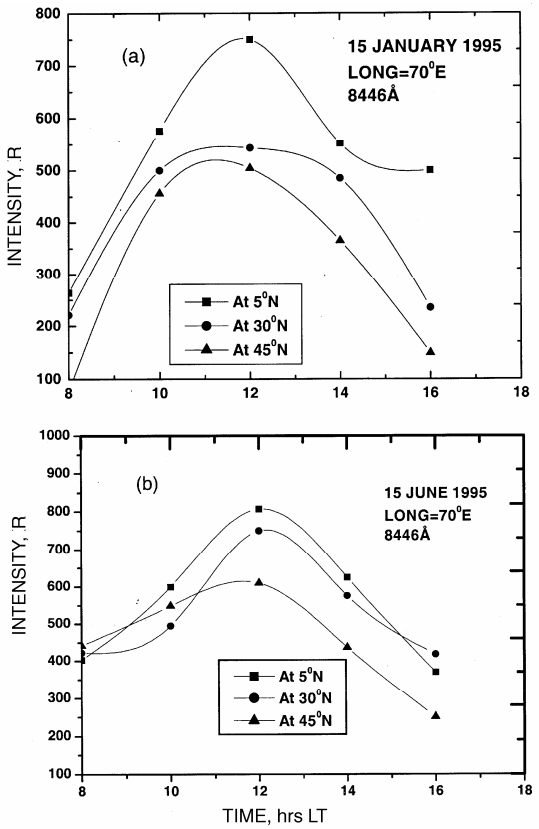

Fig. 7 — Variation of 8446 Å emission intensity as a function of local time at various latitudes for (a) 15 Jan. 1995 and (b) 15 June 1995

found lower on 15 January than on 15 June. This difference is mainly due to variation in SZA. The variation in the intensity on 15 June is about 50% whereas on 15 January it is about 30%. The peak intensity is found at local noontime (1200 hrs LT) for both the dates. The smooth variation in 8446 Å intensity may be attributed to steadiness of photoelectron fluxes at higher energies [Eqs (4) and (5)].

4 Conclusions

The emission profiles of 5577 Å, 6300 Å, 7320 Å and 8446 Å dayglow emissions have been obtained using Glow model, incorporating solar EUV flux from Tobiska[11] model. The comparison of emission rate profiles of 5577 Å and 6300 Å emissions obtained using Glow model with WINDII measurements shows a good agreement except at higher altitudes (above 160 km for 5577 Å and above 220 km for 6300 Å).

Acknowledgements

The authors thank Prof. G G Shepherd, York University, Canada, for providing the WINDII data.

One of the authors (AKU) thanks CSIR, New Delhi, for providing the financial support.

References

1 Culot F, Lathuillere C, Lilensten J & Wittase O, The OI 630.0 and 557.7 nm dayglow measured by WINDII and modeled by TRANSCAR, *Ann Geophys (France),* 22 (2004) 1.

2 Singh V & Upadhayaya A K, Greenline Dayglow Emission under Equinox conditions, *J Geophys Res (USA)*, 109 (2004) A01308.

3 Upadhayaya A K & Singh V, Correction to daytime mesospheric atomic oxygen density in MSIS-90 obtained from WINDII measurements of O(^1S) dayglow emissions, *Indian J Radio & Space Phys,* 20 (2002) 28.

4 Upadhayaya A K & Singh V, Effects of temperature dependence of reaction $N_2(A^3\Sigma_u^+)$ + O on greenline dayglow emission, *Ann Geophys (France),* 20 (2002) 2039.

5 Witasse O, Lilensten J, Lathuilere C & Blelly P L, Modeling the OI630.0 and 557.7 nm thermospheric dayglow during EISCAT-WINDII coordinated measurements, *J Geophys Res (USA)*, 104 (1999) 24639.

6 Singh V, Mcdade I C, Shepherd G G, Solheim B H & Ward W E, The O(^{1}S) dayglow emissions as observed by the WIND imaging interferometer on the UARS, *Ann Geophys (France),* 14 (1996) 637.

7 Torr D G, Torr M R & Richard P G, Thermospheric airglow emissions: A comparison of measurements from Atlas I and theory, *Geophys Res Lett (USA)*, 20 (1993) 519.

8 Kita K, Iwagami N & Ogawa T, Rocket observations of oxygen night airglow: Excitation mechanism and oxygen atom concentration, *Planet & Space Sci (UK)*, 40 (1992) 1269.

9 Solomon S C, Hays P B & Abreu V J, The auroral 6300 Å emission: Observations and modeling, *J Geophys Res (USA)*, 93 (1988) 9867.

10 Hinteregger H, Fukui E K & Gilson B R, Observational, references and model data on solar EUV, from measurements on AE-E, *Geophys Res Lett (USA)*, 8 (1981) 1147.

11 Tobiska W K, Revised solar extreme ultraviolet flux model, *J Atmos & Terr Phys (UK),* 53 (1991) 1005.

12 Bailey S M, Woods T N, Barth C A & Solomon S C, Measurements of the solar soft X-ray irradiance from the Student Nitric Oxide Explorer, *Geophys Res Lett (USA)*, 26 (1999) 1255.

13 McDade I C, Sharp W E, Richards P G & Torr D G, On the inversion of O(^{2}D-^{2}P) 7320 Å twilight airglow observations: A method for recovering both ionization frequency and the thermospheric oxygen atom densities, *J Geophys Res (USA)* 96 (1991) 259.

14 Singh V, Model calculations of OI 844.6nm emission in evening twilight, *Indian J Radio & Space Phys*, 21 (1992) 370.

15 Chang T, Torr D G, Richards P G & Solomon S C, Reevaluation of the O+(2P) reaction rate coefficients derived from atmospheric Explorer C observations, *J Geophys Res (USA)*, 98 (1993) 15589.

16 Singh V & Tyagi S, Testing of solar EUV flux models using 5577 Å, 6300 Å and 7320 Å dayglow emissions, *Adv Space Res (UK)* 30 (2002) 2557.

17 Solomon S, *Glow model version 0.95,* LASP, University of Colorado, Boulder (USA), 1992.

18 Shepherd G G,Thuiller G, Gault W A, Solheim B H, Hersom C, Alunni J M, Brun J F,Brune S, Charlot P, Cogger L L, Desauliniers D L, Evans W F J, Girod F, Gattinger R L, Harvie D, Hum R H, Kendall D J W, Llewellyn E J, Lowe R P, Ohrt J, Pasternak F, Peillet O , Powell I, Rochon Y, Ward W E, Wiens R H & Wimperis J, WINDII, the Wind Imaging Interferometer on the Upper Atmosphere Research Satellite, *J Geophys Res (USA),* 98 (1993) 10725.

19 Torr M R & Torr D G, Ionization frequencies for solar cycle 21: revised, *J Geophys Res (USA)*, 90 (1985) 6675.

20 Tyagi S & Singh V, The morphology of oxygen greenline dayglow emission, *Ann Geophys (France),* 16 (1998) 1599.

21 Link R, Dayside magnatospheric cleft auroral processes, Ph D Thesis, York University (Canada), 1982.

22 Julienne P S & Davis J, Cascade and radiation trapping effects on atmospheric atomic oxygen emission excited by electron impact, *J Geophys Res (USA)*, 81 (1976) 1397.

23 Hedin A E, Extension of the MSIS thermosphere model into the middle and lower atmosphere, *J Geophys Res (USA),* 96 (1991) 1159.

24 Rusch D W, Torr D G & Hays P B, The OII (7319–7330 A) dayglow, *J Geophys Res (USA),* 82 (1977) 719.

25 Hill S M, Solomon S C, Cleary D D & Broadfoot A L, Temperature dependence of the reaction $N_2(A^3\Sigma_u^+)$ + O in the terrestrial thermosphere, *J Geophys Res (USA)*, 105 (2000) 10615.

26 Sridharan R, Pallam Raju D, Raghavarao R & Ramarao P V S, Precursor for Equatorial Spread-F in OI 630.0 nm dayglow, *Geophys Res Lett(USA),* 21 (1994) 2797.